Astronomy & Astrophysics manuscript no.
(will be inserted by hand later)

arXiv:astro-ph/0101530v1 30 Jan 2001

On the binding energy parameter of common envelope evolution

Dependency on the definition of the stellar core boundary during spiral-in

T. M. Tauris[1] and J. D. M. Dewi[2,3,4]

[1] Nordic Institute for Theoretical Physics (NORDITA), Blegdamsvej 17, 2100 Copenhagen Ø, Denmark
e-mail: tauris@nordita.dk
[2] Astronomical Institute *Anton Pannekoek*, University of Amsterdam, Kruislaan 403, NL-1098 SJ Amsterdam, The Netherlands
[3] Bosscha Observatory, Lembang 40391, Bandung Indonesia
[4] Department of Astronomy, Institut Teknologi Bandung, Jl. Ganesha 10, Bandung 40132, Indonesia
e-mail: jasinta@astro.uva.nl

Received 9 November 2000 / Accepted 9 January 2001

Abstract. According to the standard picture for binary interactions, the outcome of binaries surviving the evolution through a common envelope (CE) and spiral-in phase is determined by the internal structure of the donor star at the onset of the mass transfer, as well as the poorly-known efficiency parameter, $\eta_{\rm CE}$, for the ejection of the H-envelope of the donor. In this Research Note we discuss the bifurcation point which separates the ejected, unprocessed H-rich material from the inner core region of the donor (the central part of the star which will later contract to form a compact object). We demonstrate that the exact location of this point is very important for evaluating the binding energy parameter, λ, which is used to determine the post-CE orbital separation.
Here we compare various methods to define the bifurcation point (core/envelope boundary) of evolved stars with masses 4, 7, 10 and 20 $\rm M_\odot$. We consider the specific nuclear energy production rate profile, the change in the mass-density gradient (Bisscheroux 1998), the inner region containing less than 10% hydrogen, the method suggested by Han et al. (1994) and the entropy profile. We also calculated effective polytropic index profiles.
The entropy profile method measures the convective boundary (at the onset of flatness in the specific entropy) which is not equivalent to the core boundary for RGB stars. Hence, this method is not applicable for RGB stars, unless the actual bifurcation point of a CE is located at the bottom of the outer convection zone (resulting in larger values of λ and larger post-CE orbital separations). On the AGB, where highly degenerate and condensed cores are formed, we find good agreement between the various methods, except for massive ($\sim 20\,\rm M_\odot$) stars.

Key words. stars: evolution – stars: mass loss – binaries: general

1. Introduction

The simple formalism introduced by Webbink (1984) and de Kool (1990) to estimate the orbital decay of binaries evolving through a CE and spiral-in evolution requires knowledge about the core mass, $M_{\rm core}$, inside the bifurcation point of the donor star as well as the λ-parameter, which is a numerical factor introduced in order to correct their simple formula for estimating the binding energy of the stellar envelope. It has been common practice to use a constant value of $\lambda = 0.5$ for the λ-parameter. We have demonstrated (Dewi & Tauris 2000) that this is not a good approach, since λ varies strongly throughout the evolution of a star. We concluded that all observations of binary pulsars originating from a CE evolution are consistent with $\eta_{\rm CE} \leq 1$, as a result of large values of λ possible when the internal thermodynamic energy is included.

We also raised the important question of *how* to define the core mass boundary – i.e. once the spiral-in process is initiated, and frictional torques deposit kinetic energy in the envelope, where is the exact location of the point of bifurcation in the envelope which separates the ejected material from the remaining condensed core region ? This question is the key issue in this Research Note. It is necessary to know $M_{\rm core}$ accurately, since it is used to determine the exact value of λ, which is a strongly increasing function exactly at the core/envelope transition. Hence, the estimates of the post-CE orbital separation also depend strongly on the value of $M_{\rm core}$.

We refer the reader to Dewi & Tauris (2000) and references therein for further details on the topic and the relevant energy equations and parameters.

Send offprint requests to: T. M. Tauris

2. Structure profiles of evolved stars

In Fig. 1 we show an example of our calculations of the stellar structure for a $10\,M_\odot$ star. The results for a 4, 7 and $20\,M_\odot$ star are summarized in Table 1. We used a chemical composition of X = 0.70 and Z = 0.02, and a mixing-length parameter of $\alpha = l/H_p = 2.0$. Convective overshooting was also taken into account. Here we used an overshooting constant of $\delta_{ov} = 0.10$ (Pols et al. 1998). We obtained almost the same core masses using $\delta_{ov} = 0.12$. For the 10 and $20\,M_\odot$ star we assumed a wind mass-loss rate according to de Jager (de Jager et al. 1988; Nieuwenhuijzen & de Jager 1990). Hence, at the tip of the AGB these two stars are estimated to have evaporated down to 9.59 and $16.2\,M_\odot$, respectively. We assumed no mass loss from the 4 and $7\,M_\odot$ stars.

We will now briefly discuss the calculations represented in Fig. 1. In the bottom panels the two solid lines show our calculations of λ. We distinguish λ_b (calculated from the total binding energy) from λ_g (as derived from gravitational binding energy alone) – see Dewi & Tauris (2000).

2.1. Energy production rate and chemical composition

A very crude definition of the stellar core region is simply as the inner part containing less than a certain mass fraction of hydrogen. As an example, we used X < 0.10 in Dewi & Tauris (2000) to define the core of the donor star. This is shown in the top panels of Fig. 1 as the area to the left of the gray shaded region. The dotted line is the core radius as a function of its mass.
A somewhat more physically meaningful approach (although not necessarily more correct in practice) is to define the core region below the (outer) shell burning source – for example, below the point of maximum energy production inside the H-burning shell. In the top panels the solid line shows the local nuclear energy production rate. The shell burning regions are clearly seen. The most abundant local chemical elements are written in the panel. As can be seen from the figure and Table 1, this definition sometimes yields significantly lower values of M_{core}.

2.2. The binding energy profile

The solid lines in the second panel are $\sinh^{-1}(\Delta W)$, where $\Delta W = E_{grav} + E_{int}$ or $\Delta W = E_{grav}$ is the binding energy of the envelope to the core (with or without the inclusion of the internal thermodynamic energy, respectively). Han et al. (1994) introduced this function to define the core mass boundary. The location is assumed to be at the transition between the strongly increasing ΔW and the outer region where ΔW varies slowly with mass. We used the intersection of straight-line fits to find M_{core}.

2.3. The mass-density gradient

The dotted line in the second panel shows the mass-density profile. The arrow indicates the point where $\partial^2 \log\rho/\partial m^2 = 0$. This criterion was used by Bisscheroux (1998) to locate the core boundary. The disadvantage of this method, from a technical point of view, is that there is not always a unique solution to the equation (for small mass steps).

2.4. The entropy profile and effective polytropic index

The entropy profile for the $10\,M_\odot$ star is plotted as a solid line in the third panel. Here "entropy" refers to the local specific entropy per baryon in units of the Boltzmann constant. The arrow indicates the sharp onset of the flat entropy gradient – another criterion for determining the bifurcation point. The core masses at the tip of the RGB, defined by this method, are always larger than those derived from other criteria. The clear discrepancy between the entropy profile method and the other alternatives on the RGB, leading to different estimates of the remaining mass after spiral-in, is easy to understand. The bifurcation point obtained from the entropy method is expected to be located further out, since it is based on the transition between the convective and the radiative layer in the stellar envelope. Unlike evolved low-mass ($1\,M_\odot$) stars, these more massive stars do not have an outer convection zone which penetrates all the way down to the H-shell near the standard core boundary region (e.g. Kippenhahn & Weigert 1990). Hence, the entropy method results in (too) large a core mass on the RGB.

The dotted line in the third panel is the "effective polytropic index" defined by: $n \equiv 1/(\gamma - 1)$ with the "adiabatic" index: $\gamma = \partial \ln P/\partial \ln \rho$. Giant stars can be considered as a condensed polytrope with a core point mass surrounded by an extended isentropic $n = 3/2, \gamma = 5/3$ envelope. Less evolved stars are more realistically described as composite polytropes consisting of $n = 3, \gamma = 4/3$ cores with $n = 3/2, \gamma = 5/3$ envelopes (Hjellming & Webbink 1987). Here, we are mostly interested in the clear discontinuous behaviour of n at the core boundary in order to determine its exact location. This discontinuity represents an important transition in the stellar structure and could be interpreted as the critical point of bifurcation at the end of the spiral-in and envelope ejection phase (cf. Section 3.2).

3. Discussion

3.1. Mass transfer initiated on the RGB vs. AGB

We have now demonstrated how different methods result in different core masses on the RGB and hence different values of λ. As an example, one can consider a $4\,M_\odot$ star at the tip of the RGB. Here the maximum energy production rate and the 10% hydrogen criterion yield core masses of 0.58 and $0.59\,M_\odot$, respectively. The mass-density gradient method results in $M_{core} = 0.68\,M_\odot$ and the outcome of applying Han et al.'s method is approximately $0.64\,M_\odot$. Using the entropy profile and the effective polytropic index method yields $M_{core} = 0.74\,M_\odot$. The spread in M_{core} from the different approaches results in: $0.6 < \lambda_b < 1.8$

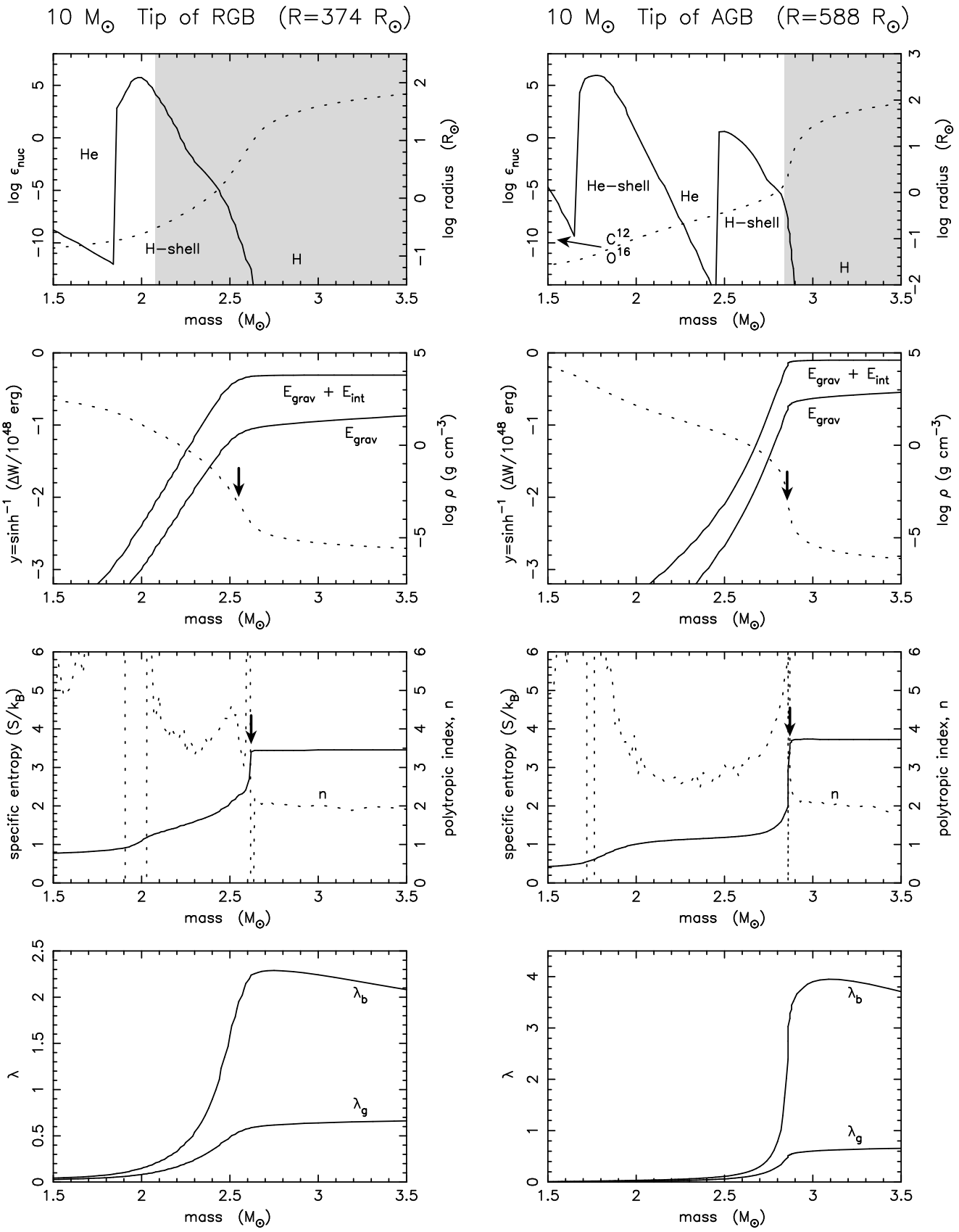

Fig. 1. The internal structure of a $10\,M_\odot$ star at the tip of the RGB (left) and at the tip of the AGB (right). See text.

Table 1. The values of $M_{\rm core}/{\rm M}_\odot$, $\lambda_{\rm g}$ and $\lambda_{\rm b}$ estimated from calculations of four different stars – see text for discussion.

	$M = 4.0\,{\rm M}_\odot$						$M = 7.0\,{\rm M}_\odot$			$M = 10.0\,{\rm M}_\odot$						$M = 20.0\,{\rm M}_\odot$		
	tip of RGB R=67 $\rm R_\odot$			tip of AGB R=1040 $\rm R_\odot$			AGB R=374 $\rm R_\odot$			tip of RGB R=374 $\rm R_\odot$			tip of AGB R=588 $\rm R_\odot$			tip of AGB R=1040 $\rm R_\odot$		
method	$M_{\rm core}$	$\lambda_{\rm g}$	$\lambda_{\rm b}$	$M_{\rm core}$	$\lambda_{\rm g}$	$\lambda_{\rm b}$	$M_{\rm core}$	$\lambda_{\rm g}$	$\lambda_{\rm b}$	$M_{\rm core}$	$\lambda_{\rm g}$	$\lambda_{\rm b}$	$M_{\rm core}$	$\lambda_{\rm g}$	$\lambda_{\rm b}$	$M_{\rm core}$	$\lambda_{\rm g}$	$\lambda_{\rm b}$
max $\epsilon_{\rm nuc}$	0.58	0.32	0.62	1.37	0.91	—	1.58	0.10	0.20	1.99	0.09	0.13	2.47	0.06	0.10	6.80	0.02	0.05
X < 0.10	0.59	0.36	0.70	1.37	0.91	—	1.80	0.59	2.85	2.08	0.11	0.21	2.84	0.40	1.80	6.80	0.02	0.05
$\partial^2 \log\rho/\partial m^2 = 0$	0.68	0.66	1.60	1.37	0.91	—	1.80	0.59	2.85	2.54	0.54	1.80	2.85	0.46	2.20	7.50	0.22	0.95
Han et al.	0.64	0.59	1.17	1.37	0.91	—	1.80	0.59	2.85	2.52	0.51	1.75	2.85	0.46	2.20	7.60	0.32	1.70
entropy profile	0.74	0.73	1.81	1.37	0.91	—	1.80	0.59	2.85	2.62	0.60	2.23	2.86	0.55	3.20	7.80	0.45	3.50

and $0.3 < \lambda_{\rm g} < 0.75$ (with and without internal thermodynamic energy). If we now assume the simple CE energy equations (Webbink 1984; de Kool 1990) to be approximately valid, and this $4\,{\rm M}_\odot$ ($R = 67\,{\rm R}_\odot$) star is in a common envelope with an in-spiralling $1.3\,{\rm M}_\odot$ neutron star, the evolution would then result in a final post-CE orbital separation of 0.70 or $2.75\,{\rm R}_\odot$, for $M_{\rm core} = 0.58$ and $0.74\,{\rm M}_\odot$, respectively. Here we assumed $\lambda = \lambda_{\rm b}$, $\eta_{\rm CE} = 1.0$ and no significant accretion onto the neutron star during spiral-in. However, the core radius of the stripped star is $0.1\,{\rm R}_\odot$ ($M_{\rm core} = 0.58\,{\rm M}_\odot$) or $3.5\,{\rm R}_\odot$ ($M_{\rm core} = 0.74\,{\rm M}_\odot$). Hence, in the latter case, the large core would then have a radius larger than the predicted post-CE separation. Therefore this system would coalesce during the spiral-in – perhaps leaving behind a black hole. Assuming $\lambda = \lambda_{\rm g}$ (i.e. considering gravitational binding energy alone), or choosing a small efficiency parameter (e.g. $\eta_{\rm CE} = 0.3$), would decrease the predicted post-CE separation still further and lead to an earlier coalescense. We conclude that knowledge of the accurate bifurcation boundary is crucial to forecast the outcome of a CE evolution on the RGB.

Many binaries come into contact while the donor star is expanding enormously on the AGB. If we consider the same $4\,{\rm M}_\odot$ star as before, but now at the tip of the AGB, *all* methods yield *exactly* the same core mass. For the 7 and $10\,{\rm M}_\odot$ stars on the AGB, the different methods also yield the same core mass (except for the location of the maximum energy production rate in the H-shell, which is below this boundary at the outer edge of the shell source). It is important to notice the fact that the envelope binding energy is a strongly increasing quantity near/at the core boundary on the AGB. Hence, the resulting values of λ are also increasing sharply at this transition (see Fig. 1). Since the material of the donor star is peeled off from the outside, we suggest using the (larger) value of lambda at the mesh point, just outside the bifurcation point.

3.2. Envelope ejection process

While the location of the bifurcation point, separating the ejected envelope from the condensed core region, is straightforward to define on the AGB, it is important to know for RGB stars if the envelope of the evolved donor is ejected at the bottom of the convection zone, or closer to the stellar center at the core boundary near/at the outer shell source (surrounding the inner part of the star). For convective material in an isentropic envelope, $R \propto M^{-1/3}$ and thus removal of envelope mass causes the star to expand. Therefore, in a CE system, the envelope is easily peeled off until the entropy profile increases outwards (in the deeper radiative layers). From this point on the star will no longer expand and the envelope may already be separated from the inner region, depending on the details of the ejection process. It would be interesting to see if multi-dimensional hydrodynamical calculations could answer this question.

Binaries which come into Roche-lobe contact early in the stellar evolution of the donor will not survive the spiral-in process at all (there is simply not enough orbital energy available to expel the envelope).

The values of λ presented in Table 1 in Dewi & Tauris (2000) were calculated from the 10% hydrogen criterion. From the work presented here we can see that these values should therefore be taken as *minimum* values of λ, supporting our previous conclusion that $\eta_{\rm CE}$ need not be large since the value of λ itself is expected to be large.

Acknowledgements. We thank the referee for improving (but substantially shortening) this paper. T. M. T. acknowledges the receipt of a NORDITA fellowship. This work was sponsored by NWO Spinoza Grant 08-0 to E. P. J. van den Heuvel.

References

Bisscheroux B., 1998, M.Sc. Thesis, Univ. Amsterdam
de Jager C., Nieuwenhuijzen H., van der Hucht K. A., 1988, A&AS 72, 259
de Kool M., 1990, ApJ 358, 189
Dewi J. D. M., Tauris T. M., 2000, A&A 360, 1043
Han Z., Podsiadlowski P., Eggleton P. P., 1994, MNRAS 270, 121
Hjellming M. S., Webbink R. F., 1987, ApJ 318, 794
Kippenhahn R., Weigert A., 1990, Stellar Structure and Evolution, A&A Library, Springer-Verlag
Nieuwenhuijzen H., de Jager C., 1990, A&A 231, 134
Pols O. R., Schröder K.-P., Hurley J. R., Tout C. A., Eggleton P. P. , 1998, MNRAS 298, 525
Webbink R. F., 1984, ApJ 277, 355